nature communications

Article

https://doi.org/10.1038/s41467-024-52690-y

Fluoropolymer sorbent for efficient and selective capturing of per- and polyfluorinated compounds

Received: 10 July 2024

Accepted: 19 September 2024

Published online: 27 September 2024

Check for updates

Zhuojing Yang[1,2], Yutong Zhu[1,2], Xiao Tan[1,2], Samruddhi Jayendra Jayendra Gunjal[1,2], Pradeep Dewapriya[3], Yiqing Wang[1,2], Ruijing Xin[1], Changkui Fu[1], Kehan Liu[1,2], Katie Macintosh[4], Lee G. Sprague[5], Lam Leung[5], Timothy E. Hopkins[5], Kevin V. Thomas[3], Jianhua Guo[6], Andrew K. Whittaker[1,7] & Cheng Zhang[1,2]

Per- and poly-fluoroalkyl substances (PFAS) have gained widespread attention due to their adverse effects on health and environment. Developing efficient technology to capture PFAS from contaminated sources remains a great challenge. In this study, we introduce a type of reusable polymeric sorbent (PFPE-IEX +) for rapid, efficient, and selective removal of multiple PFAS impurities from various contaminated water sources. The resin achieves >98% removal efficiency ([PFPE-IEX +] = 0.5–5 mg mL^{-1}, $[PFAS]_0$ = 1–10 ppb in potable water and landfill leachate) and >500 mg g^{-1} sorption capacity for the 11 types of examined PFAS. We achieve efficient PFAS removal without breakthrough and subsequent resin regeneration and demonstrate good PFAS recovery in a proof-of-concept cartridge setup. The outcomes of this study offer valuable guidance to the design of platforms for efficient and selective PFAS capture from contaminated water, such as drinking water and landfill leachate.

Per- and poly-fluoroalkyl substances (PFAS) are a large group of synthetic chemicals that have been widely used in various applications[1–3]. However, the widespread use of PFAS has led to their ubiquitous presence in the environment, as well as concerns about their potential adverse effects on human health and the environment[4,5]. In addition, the economic costs of PFAS contamination encompass a wide array of expenses, including those related to water treatment, environmental remediation, healthcare for affected populations, and potential legal liabilities for industries responsible for PFAS pollution. These financial burdens highlight the significant economic implications of PFAS contamination and underscore the urgent need for effective remediation strategies to mitigate these costs and protect public health and the environment[6].

Conventional concentration technologies, including the use of granular activated carbons[7], ion-exchange resins[8] and foam fractionation[9], are commonly employed for the removal of PFAS from contaminated water sources. However, the efficiency of these technologies can be reduced in several ways[10,11]. First, competitive sorption by other contaminants significantly impacts sorption capacity. Conventional remediation technologies typically remove waterborne contaminants nonspecifically, resulting in rapid saturation by nonfluorinated species thus significantly reducing

[1]Australian Institute for Bioengineering and Nanotechnology, The University of Queensland, Brisbane QLD 4072, Australia. [2]The Centre for Advanced Imaging (CAI), The University of Queensland, Brisbane QLD 4072, Australia. [3]Queensland Alliance for Environmental Health Sciences, The University of Queensland, Level 4, 20 Cornwall Street, Woolloongabba, QLD 4102, Australia. [4]City of Gold Coast 833 Southport Nerang Rd, Nerang QLD 4211, Australia. [5]The Chemours Company, Chemours Discovery Hub, 201 Discovery Boulevard, Newark, DE 19713, USA. [6]Australian Centre for Water and Environmental Biotechnology, The University of Queensland, St. Lucia, QLD, Australia. [7]Australian Research Council Centre of Excellence for Green Electrochemical Transformation of Carbon Dioxide, The University of Queensland, Brisbane, Australia. e-mail: c.zhang3@uq.edu.au

sorption capacity[12–16]. Second, removal of short-chain PFAS by conventional technologies is significantly less effective. For example, the aeration-foam fractionation technology allows 96% removal efficiency for long-chain perfluorooctanesulfonic acid (PFOS), while only 50% for perfluorohexanesulfonic acid (PFHxS) and 30% for perfluorobutanesulfonic acid (PFBS) (initial concentration for each $[PFAS]_0 = 0.093$ mmol L^{-1} with a flow rate of 75 mL min^{-1})[17]. Granular activated carbons (GAC) also show low HFPO-DA (or GenX, the ammonium salt of hexafluoropropylene oxide dimer acid) and heptafluorobutyric acid (PFBA) removal efficiency at <40%, and 50–60% for perfluorooctanoic acid (PFOA, $[GAC] = 10$ mg L^{-1}, $[PFAS]_0 = 1$ ug L^{-1})[18].

Partially fluorinated polymer sorbents have been reported by us and other groups to sorb PFAS from contaminated water with high efficiency and selectivity[18–22]. The high affinity between PFAS and fluoropolymers is due to specific fluorous interactions, which overcome the major challenge of competitive sorption of other dissolved co-contaminants[19]. The Leibfarth group[18,23] utilized flexible perfluoropolyethers (PFPE, T_g of ~ −90 °C) as the fluorinated core, leading to improved capacity at 278 mg g^{-1} for HFPO-DA. PFPEs are amorphous, low-molecular-weight perfluorinated oligomers synthesized from the gas phase without the use of perfluorinated acid surfactants[24,25]. They exhibit greater susceptibility to degradation (e.g. thermal degradation in the presence of Lewis acids (metal oxides and halides)) compared to perfluorocarbons when they reach the end of their useful lifespan[26]. The thermal degradation of PFPE does not produce environmentally concerning perfluorinated acids but primarily results in low molecular weight oligomers, such as polymer fragments containing fluorocarbonyl end groups, difluoromethane, and metal fluoride[26]. In addition, it is worth noting that despite the improvement in sorption achieved using PFPE as the fluorinated segments, the fundamental investigations into how the microstructures of PFPE segments may influence PFAS capture, as well as the effective management of the recycled PFAS wastes, remain largely unexplored.

In this study, we introduce a PFAS capture technology that utilizes reusable PFPE-modified polystyrenic ion-exchange sorbents, designated as PFPE-IEX+. We choose the low-molecular-weight PFPE ($M_n \approx 2000$ g mol^{-1} with a repeating chain length of ~ 11) for its ease of handling and solubility in common organic solvents, facilitating chemical modification and polymerization processes. Superior removal efficiency, kinetics, capacity and regenerability for multiple PFAS in both potable water and landfill leachate were demonstrated in batch and cartridge experiments. Our results suggest that the reusable PFPE-IEX+ sorbents are efficient in the removal of multiple PFAS chemicals from contaminated water sources.

Results and discussion

PFPE-IEX+ design and synthesis

The typical chemical structure and synthetic routine of PFPE-IEX+ are shown in Fig. 1a. Styrenically functionalized perfluoropolyether (sPFPE) were firstly synthesized through alkylation reaction between PFPE-OH and 4-vinylbenzyl chloride (VBC)[27]. Both ^{1}H and ^{19}F NMR spectra of sPFPE confirm the successful synthesis of the sPFPE monomer (colorless oil), as all the peaks have been successfully assigned, and are shown in Fig. 1b and Supplementary Fig. 1. PFPE-IEX (white powder) was then synthesized and confirmed by performing solid-state (SS) ^{13}C NMR and Fourier-transform infrared spectroscopy (FTIR). Quaternary ammonium group was obtained using trimethylamine to produce cationic PFPE-containing white gel PFPE-IEX+. The successful formation of quaternary ammonium group was again confirmed by SS ^{13}C NMR (Fig. 1c) and FTIR (Fig. 1d). In the SS ^{13}C NMR spectrum, the carbon atoms belonging to the -CH_2-Cl group of PFPE-IEX shift from ~ 40 (peak c) to ~ 50 ppm (peak f) after introducing quaternary ammonium group[28,29]. Additionally, the newly formed sharp peak at 68 ppm is due to the carbon atom from the -N-$(CH_3)_3$ group. FTIR further confirms the successful quaternization of the PFPE-IEX resin, with typical absorption peaks at 3005 cm^{-1}, 1474 cm^{-1}, and 895 cm^{-1} appearing, assigned to the C-H bending and stretching of trimethyl group from quaternary ammonium cations (Fig. 1d)[30,31]. The above results demonstrate the successful preparation of PFPE-IEX and subsequent introduction of quaternary ammonium group to produce PFPE-IEX+ (size 80–100 μm, Fig. 1e).

The swelling ratio is an important additional consideration to confirm the availability of sorbent to achieve long-term continuous PFAS removal in cartridges. Out of the three prepared sorbents (Supplementary Table 1), each possessing varying crosslinker DVB contents (4, 10 and 20 wt%), the 10 wt% sorbent demonstrated a favorable swelling ratio of 6%, indicating a moderate level of swelling (Supplementary Fig. 2). Consequently, we have opted to utilize this 10 wt% PFPE-IEX+ sorbent for the subsequent tests. The polystyrene matrix of PFPE-IEX+ also shows good stability in both acidic and alkaline conditions, minimizing hydrolysis in aqueous solutions (Supplementary Figs. 3–6). Small-angle X-ray scattering (SAXS) experiment on the swollen PFPE-IEX+ reveals a broad peak at ~$q = 0.07$ $Å^{-1}$ (Supplementary Fig. 7). This indicates the presence of aggregate clusters, likely originating from the PFPE segments, potentially further contributing to PFAS capture through fluorous interaction between PFPE clusters and fluorinated PFAS tails (Fig. 1f)[20,21].

Equilibrium sorption

The removal efficiency of 11 different PFAS, including short-chain perfluoroalkyl carboxylic acids (PFCAs, $C_nF_{2n+1}COOH$, $n < 7$) and perfluoroalkyl sulfonic acids (PFSAs, $C_nF_{2n+1}SO_3H$, $n < 6$), long-chain PFCA ($n \geq 7$) and PFSA ($n \geq 6$)[32,33], and one major emerging PFAS, ammonium salt of hexafluoropropylene oxide dimer acid (HFPO-DA or GenX) was tested using PFPE-IEX+ determined by liquid chromatography with tandem mass spectrometry (LC-MS/MS, Supplementary Fig. 8). Two commercially available sorbents were used as controls, including granular activated carbon (GAC, 20–40 mesh particle size) and anion exchange resin (IEX, Amberlite IRA-410, 20–25 mesh particle size). The addition of 20 mg L^{-1} (ppm) of humic acid and 200 mg L^{-1} of sodium chloride (NaCl) was to simulate the natural PFAS contaminated environment. It is worth noting that in real engineering system, sorbents may be preloaded with natural organic matter, potentially impacting PFAS sorption performance. However, the incorporation of PFPE segments in our sorbents is specifically targeted to minimize such influences. An initial concentration of 100 μg L^{-1} (ppb) for each PFAS was chosen to simulate concentrations found in landfill leachate, which is a primary focus of the study.

After treatment for 24 h, >99% removal efficiency for all tested PFAS (>98% for PFBA) was achieved, highlighting the superior removal efficiency of PFPE-IEX+ for capturing PFAS compared with commercially available GAC and IEX sorbents (Fig. 2b). To be more specific, PFPE-IEX+ shows >99.5% removal of HFPO-DA after 24 h of incubation, which is significantly higher compared to that treated by GAC and IEX (83.5% and 35%, respectively). In comparison to previous reported sorbents, PFPE-IEX+ resin exhibits significantly higher PFAS removal efficiency, especially for short-chain PFAS. For example, styrene-functionalized β-cyclodextrin (StyDex) polymers removes ~ 95% of PFHxS[34], amine-containing β-cyclodextrin polymer captures ~ 70% of HFPO-DA and ~ 40% of PFBA[35], and quaternary ammonium covalent organic frameworks sorb ~ 60% of PFHxS[36], all of which are lower than the removal efficiency of PFPE-IEX+.

Sorption kinetics

The results presented in Fig. 2c demonstrate that all 11 PFAS could be efficiently removed (>85% in <30 s and >99% in 120 min), highlighting the rapid recognition and efficient removal of PFAS compounds using PFPE-IEX+ sorbent. It should be noted that no desorption occurred throughout the entire 120 min sorption period, indicating the robust

https://doi.org/10.1038/s41467-024-52690-y

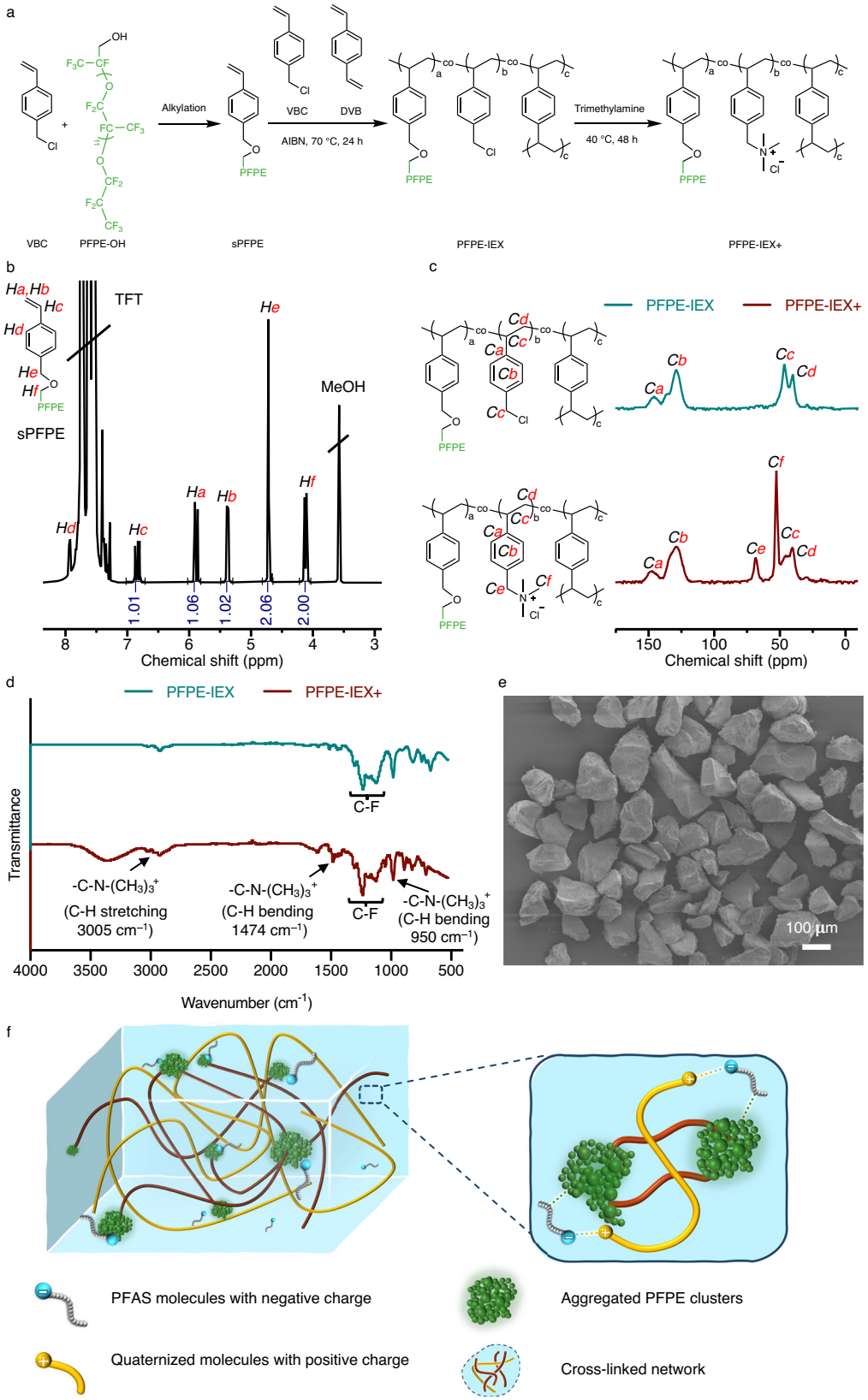

Fig. 1 | Synthesis and characterization of PFPE-IEX and PFPE-IEX+ resins. **a** Chemical structure and synthetic scheme for PFPE-IEX+ sorbent. **b** ^{1}H NMR spectrum and corresponding assignment of sPFPE in $CDCl_3$. **c** Solid-state ^{13}C NMR spectra and (**d**) FTIR spectra of PFPE-IEX and PFPE-IEX+ indicate the successful preparation of resins. **e** Morphology of PFPE-IEX+ acquired under SEM. **f** Schematic illustration of interactions between PFAS compounds with PFPE aggregate cluster and quaternary ammonium group within PFPE-IEX + .

https://doi.org/10.1038/s41467-024-52690-y

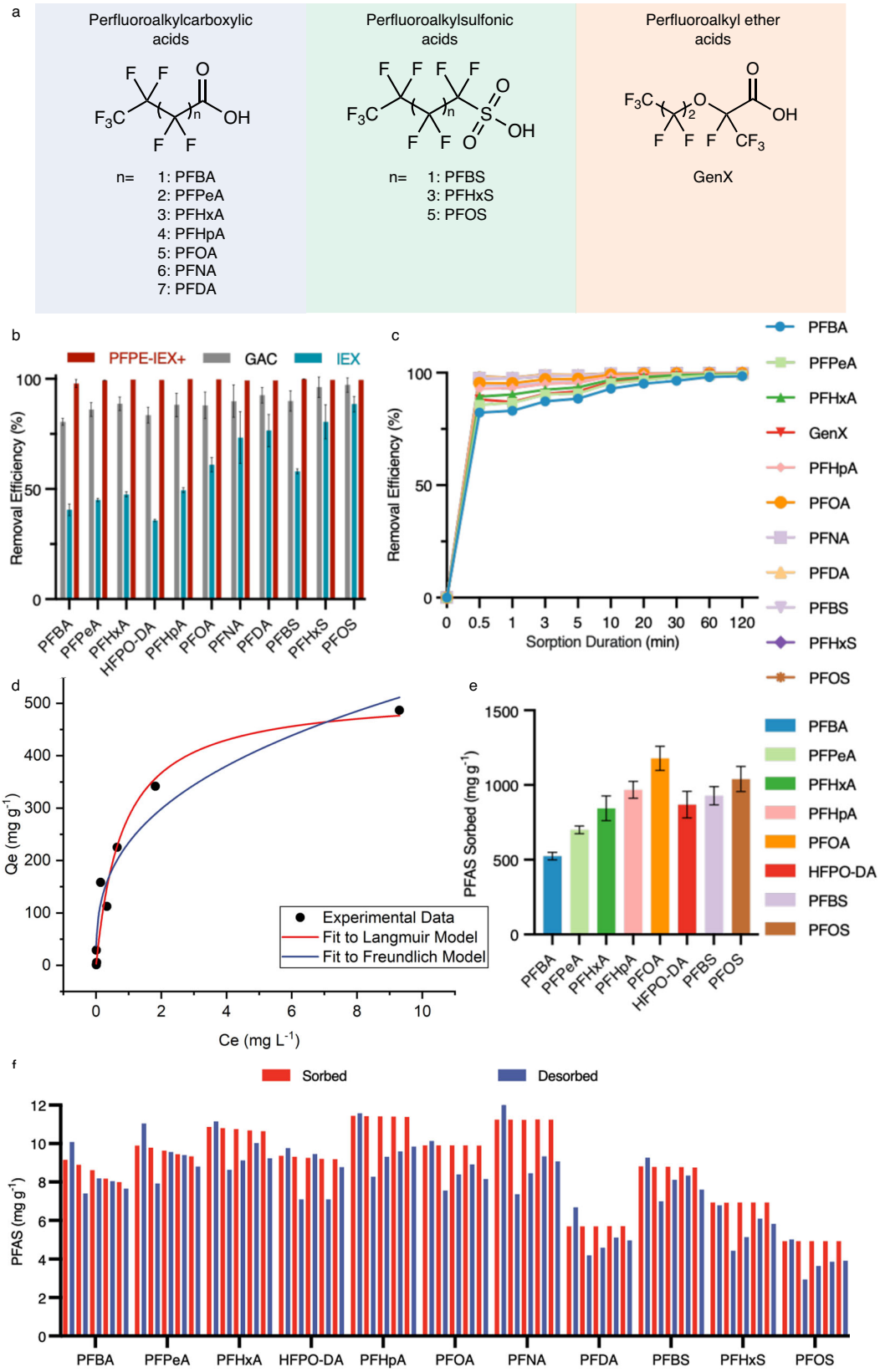

binding between PFAS and PFPE-IEX+ via fluorous and hydrophobic interactions and electrostatic attraction.

Sorption capacity

Sorption isotherm of PFAS using PFPE-IEX+ resin was performed to understand the binding mechanisms between PFAS and PFPE-IEX + . As shown in Fig. 2d, the sorption data was fitted by the Langmuir and Freundlich models using equations shown in the Methods section, using non-linear curve fittings[37–40]. The isotherm parameters for both models are listed in Table 1. The Langmuir model has a better fit than the Freundlich model with a higher R^2 value (0.9493 vs. 0.9333). The calculated K_L and q_m are $1.21 \times 10^5\,M^{-1}$ and 518.9 mg g^{-1}, respectively,

Fig. 2 | Sorption efficiency, kinetics, capacity and regeneration of PFPE-IEX + . **a** Chemicals structure of 11 types of PFAS used in this study. **b**, Removal efficiency of 11 PFAS treated PFPE-IEX+ (red), GAC (gray) and IEX (light blue) for 24 h. Sorbent concentration, 0.5 mg mL^{-1}; PFAS initial concentration, 100 ppb each. Water constituents, milli-Q water with the presence of NaCl (200 ppm) and humic acid (20 ppm), pH = 5.0. The error bars denote standard deviations, where $n = 3$. **c** Sorption kinetics using PFPE-IEX+ in milli-Q water. Sorbent concentration, 0.1 mg mL^{-1}; PFAS initial concentration, 100 ppb each. **d** Binding isotherm study between HFPO-DA and PFPE-IEX + . Sorbent concentration, 0.1 mg mL^{-1}; HFPO-DA concentration, 0.1–50 ppm; sorption duration, 24 h. **e** Individual capacity of eight different PFAS of PFPE-IEX+ determined by ^{19}F NMR. Sorbent concentration, 0.2 mg mL^{-1}; PFAS concentration, 0.4 mg mL^{-1} each in Milli-Q water; Sorption duration, 24 h. The error bars denote standard deviations, where $n = 3$. **f** Regeneration performance for multiple PFAS using PFPE-IEX+ determined by LC-MS/MS (sorbed (red); desorbed (blue)). Sorbent concentration, 1 mg mL^{-1}; $[PFAS]_0 = 10$ ppm; sorption and desorption duration, 30 min. The variations in sorption capacity in mg g^{-1} are attributed to the differing initial concentrations of each PFAS.

indicating a strong binding affinity between HFPO-DA and PFPE-IEX+ sorbent. This further supports the observations in the above section, specifically the absence of desorption within the tested time period. The sorption capacity of HFPO-DA at 518.9 mg g^{-1} is significantly higher compared to that of previously reported sorbents under equivalent testing conditions (e.g. crosslinked β-cyclodextrin-containing polymer ($K_L = 8.8 \times 10^4\ M^{-1}$, $q_m = 222.0$ mg g^{-1})[35], chitosan modified adsorbent ($q_m = 364.6$ mg g^{-1})[41], fluorogels ($K_L = 5.9 \times 10^6\ M^{-1}$, $q_m = 278.0$ mg g^{-1})[18], fluorinated hydrogels ($q_m = 34.2$ mg g^{-1})[42], covalent organic frameworks ($K_L = 6.3 \times 10^4\ M^{-1}$, $q_m = 200.0$ mg g^{-1})[19], and magnetic PFPE sorbents ($K_L = 4.8 \times 10^5\ M^{-1}$, $q_m = 219$ mg g^{-1})[43]. The maximum sorption capacity of PFPE-IEX+ for the removal of seven other types of PFAS, i.e. PFBA, perfluoro-n-pentanoic acid (PFPeA), perfluorohexanoic acid (PFHxA), perfluoroheptanoic acid (PFHpA), PFOA, PFBS and PFOS, were also tested in Milli-Q water (Supplementary Fig. 9 and Fig. 2e), indicating the sorption capacities for all tested PFAS using PFPE-IEX+ are significantly higher compared with previously reported sorbents (please see detailed discussion in the Supplementary Information).

Sorbent regeneration

Sorbent regeneration is a key factor in evaluating the practicality of PFAS sorbents. HFPO-DA was again chosen as a representative PFAS to demonstrate the regeneration of PFPE-IEX + . Five cycles that include both sorption and desorption experiments were performed by alternating between aqueous and methanol+NaCl solutions (Fig. 2f and Supplementary Fig. 10)[23,43,44]. Both ^{19}F NMR and LC-MS/MS were performed for characterization of the sorption/desorption of HFPO-DA by PFPE-IEX+. Efficient removal of HFPO-DA was achieved in the first sorption cycle (>99% removal efficiency with capacity of 173 and 174 mg g^{-1} determined by ^{19}F NMR and LC-MS/MS, respectively), followed by efficient desorption and release of HFPO-DA in methanolic salt solution.

In addition, we tested the adsorbent regeneration of multiple PFAS, as shown in Fig. 2f and Supplementary Fig. 11, demonstrating efficient desorption and release for all types of PFAS tested. However, it was observed that the desorption efficiency of HFPO-DA was not as high as in the sorption step, likely due to the limited solubility of HFPO-DA in methanol at high concentrations and/or the potential inefficacy of NaCl in disrupting the electrostatic binding between PFAS and the sorbent. Nevertheless, PFPE-IEX+ maintains a good sorption efficiency of>90% over five cycles for all 11 PFAS without a significant loss in sorption capacity, demonstrating that PFPE-IEX+ is regenerable for repeated PFAS removal.

PFAS removal in real-life PFAS contaminated water

The sorption performance using PFPE-IEX+ was further tested in PFAS contaminated potable water and landfill leachate, and compared with commercially available GAC. The total organic carbon (TOC) of landfill leachate was 624.3 mg L^{-1}, while that of potable water was non-detectable (<0.1 mg L^{-1}). Metal ion concentrations for both water matrices were quantified using inductively-coupled plasma optical emission spectrometry (ICP-OES) and the results are shown in Supplementary Table 2. Both water matrices were spiked with 11 different PFAS, with each PFAS having an initial concentration of low ppb level (1-10 ppb), followed by individual treatment for 24 h using PFPE-IEX+ and GAC. The results in Fig. 3a demonstrate that both sorbents show efficient removal of all PFAS in potable water, i.e. the solution with low levels of co-contaminants.

When treating the PFAS contaminated leachate using PFPE-IEX+ or GAC at the same sorbent concentration of 5 mg mL^{-1}, the results in Fig. 3b demonstrate that PFPE-IEX+ shows significantly higher removal of all of the 11 PFAS compared with GAC. For example, after treatment by PFPE-IEX+, high removal efficiency of the majority of the PFAS species was still maintained, with >99% removal for short chain PFAS including PFHxA, PFHpA and PFBS, >98% removal of all long chain PFAS tested and > 99% removal of HFPO-DA being observed. In contrast, GAC shows only 30% to 40% of the short-chain PFAS and only 40% of HFPO-DA, presumably due to interference from the complex components i.e. co-contaminants present in the leachate.

The sorption kinetics of 11 spiked PFAS at an environmentally relevant concentration (2 ppb) were further investigated using PFPE-IEX+ at two different sorbent concentrations of 0.5 and 5 mg mL^{-1} in leachate. The results shown in Fig. 3c demonstrate that perfluorodecanoic acid (PFDA) and PFOS were effectively removed (> 99% with 0.5 mg mL^{-1} PFPE-IEX+) within 30 s, while for the PFAS with shorter chain lengths, at least 5 min was needed for the sorption to reach equilibrium.

For the sorbent at higher concentration i.e. 5 mg mL^{-1}, fast removal of the PFAS was observed except for PFBA (Fig. 3d), indicating rapid recognition of the PFAS by PFPE-IEX+ without significant interference from the other components of the leachate. The enhanced sorption kinetics observed at higher sorbent concentrations could be attributed to the following factors: (1) there are more active sites available for PFAS molecules to adsorb onto at higher concentrations. This increased availability of active sites can lead to faster initial sorption rates; (2) at higher concentrations of sorbents, there may be a higher density of sorbent particles in the solution, leading to a higher collision frequency between PFAS molecules and the sorbent surface. This increased collision frequency can result in faster sorption kinetics.

The data presented in Fig. 3c were analyzed using the Weber-Morris model (see the Methods section for details) to elucidate the intraparticle diffusion effect during sorption. As illustrated in Fig. 3e and Supplementary Table 3, the fitted lines exhibit low linearity (indicated by low R^2 values) and high y-axis intercepts, suggesting that intraparticle diffusion was not the rate-limiting step in PFAS sorption using PFPE-IEX+. The reduced hindrance to transfer associated with intraparticle diffusion in PFPE-IEX+ could enhance the sorption kinetics[45].

Table 1 | Langmuir and Freundlich constants for the sorption of HFPO-DA using PFPE-IEX +

Langmuir			Freundlich		
K_L (M^{-1})	q_m (mg g^{-1})	R^2	K_F ((mg g^{-1})(L mg^{-1})$^{1/n}$)	n	R^2
1.21x10^5	518.9	0.9493	234.4	2.858	0.9333

Continuous PFAS removal and regeneration in a cartridge

Encouraged by the above performance of PFPE-IEX+ in the removal of PFAS from real PFAS contaminated water, we then proceeded to

https://doi.org/10.1038/s41467-024-52690-y

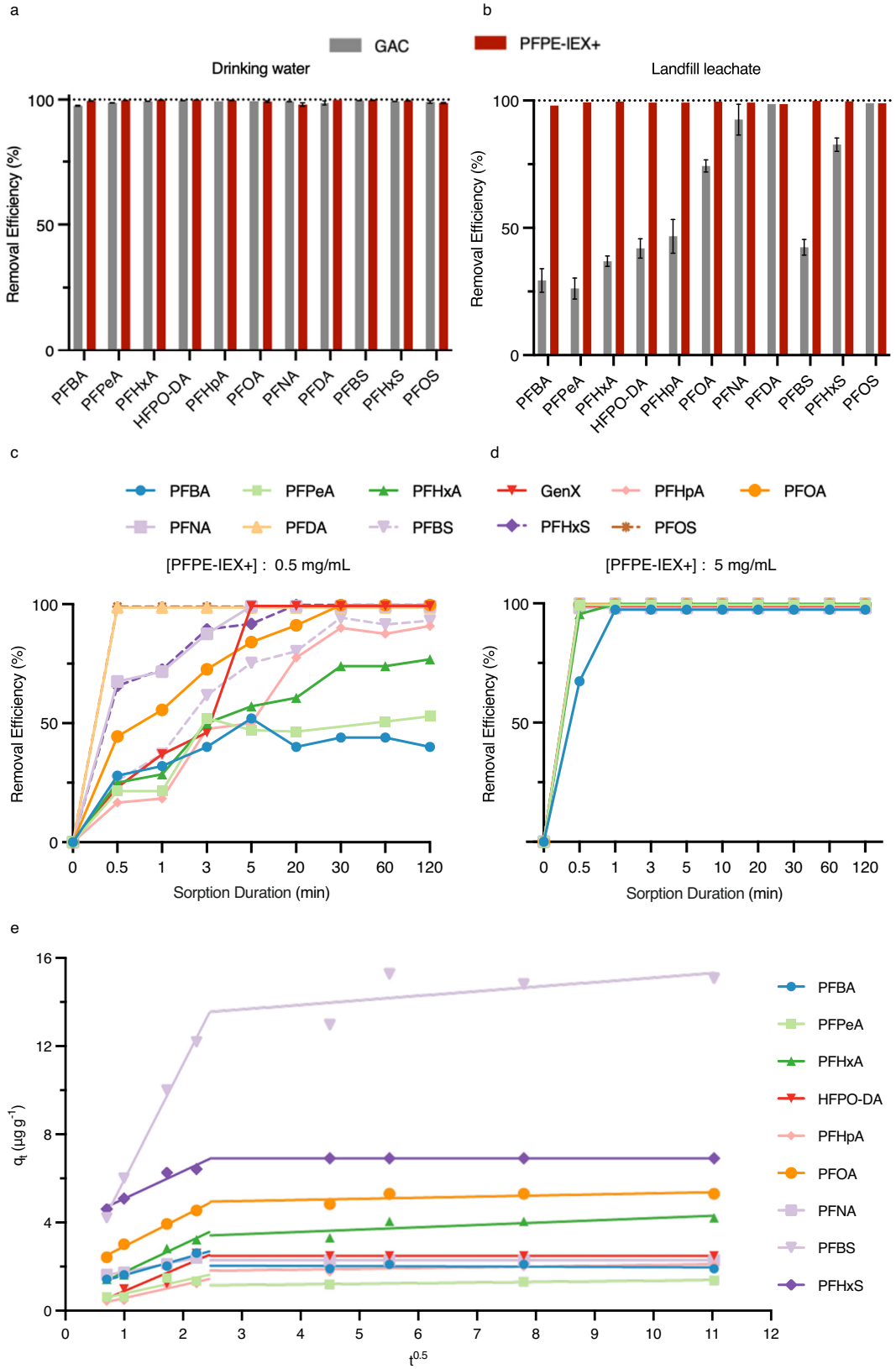

Fig. 3 | PFAS removal performance in real contaminated potable water and landfill leachate water. a Multiple PFAS removal efficiency using GAC (gray) and PFPE-IEX+ (red) in potable water. Sorbent concentration 5 mg mL^{-1}; PFAS initial concentration 1–2 ppb each; sorption time 24 h. **b** Multiple PFAS removal using GAC (gray) and PFPE-IEX+ (red) in leachate. Sorbent concentration 5 mg mL^{-1}; PFAS initial concentration 1–10 ppb each; sorption time 24 h. The error bars in a,b denote standard deviations, where $n = 3$. **c**,**d**, Sorption kinetics using PFPE-IEX+ in leachate with sorbent concentration at (**c**) 0.5 mg mL^{-1} and (**d**) 5 mg mL^{-1}. PFAS initial concentration, 1–10 ppb each. **e** The fitting of kinetics data shown in Fig. 3c using Weber-Morris intraparticle diffusion model. Source data are provided as a Source Data file.

https://doi.org/10.1038/s41467-024-52690-y

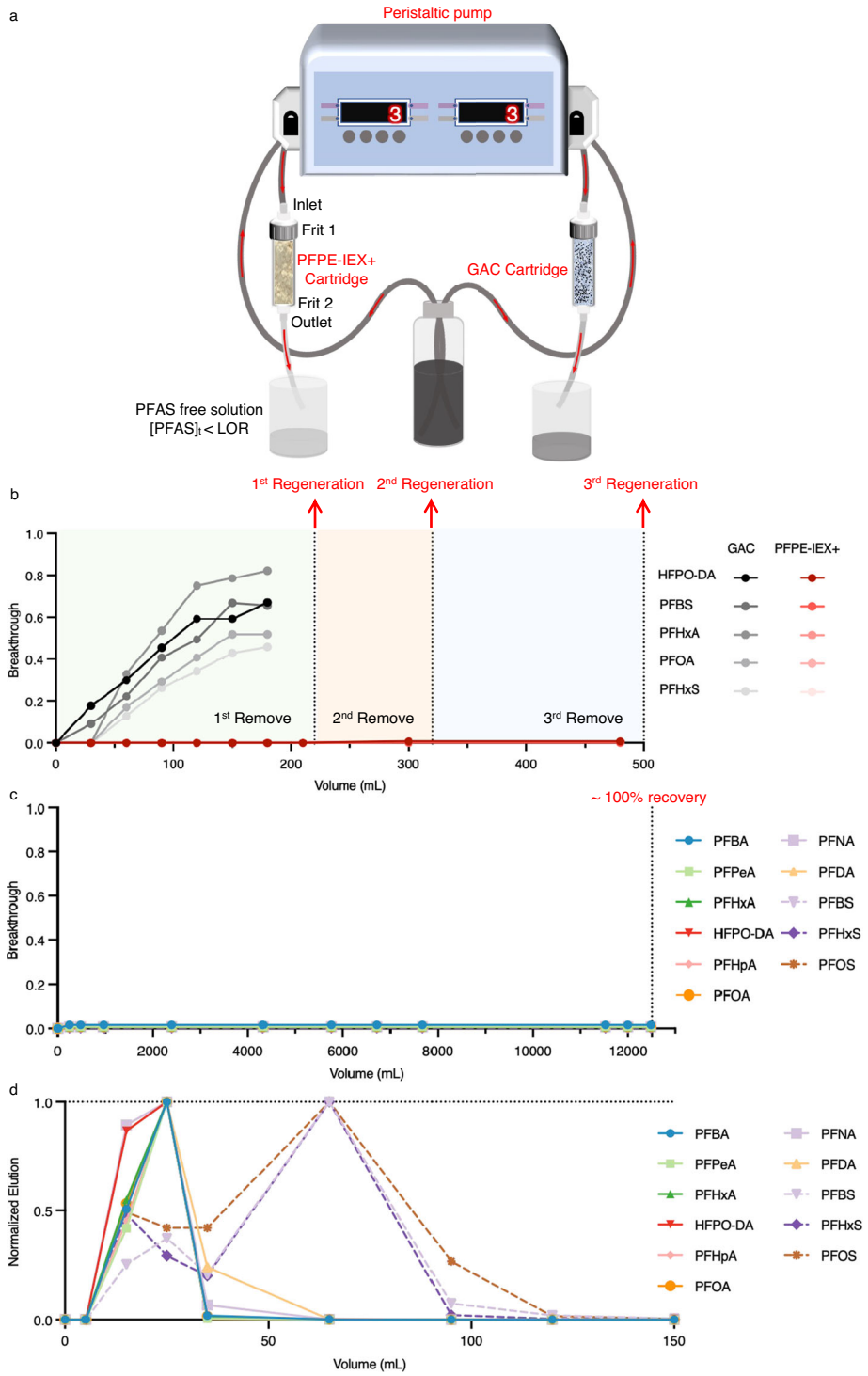

Fig. 4 | Continuous PFAS removal and sorbent regeneration in cartridges. **a** Each cartridge contains 2 g of sorbents. The water flow speed is controlled by a peristaltic pump set to 3 mL min^{-1}. LOR represents limit of reporting. **b**, **c** PFAS remove performance using column (**b**) in leachate, PFAS initial concentration 1–10 ppb each; (**c**) in potable water, PFAS initial concentration 1–2 ppb each. The breakthrough curve for the column was determined by plotting the ratio of the $[PFAS]_t/[PFAS]_0$ against the elution volume ($[PFAS]_t$ and $[PFAS]_0$ are each PFAS concentration of effluent and influent, respectively). The observation of 10% breakthrough can be used as an indication that early breakthrough is observed[23,46]. **d** Column PFAS regeneration performance in potable water. Extraction solution: 1% NaCl in methanol. The normalization of PFAS concentration was carried out by dividing each data point by the maximum concentration value.

develop a cartridge for removal of PFAS in a continuous process (Fig. 4a). For the PFPE-IEX+ sorbent, no breakthrough of PFAS was observed even after three removal and regeneration cycles (Fig. 4b). In contrast, the GAC sorbent showed high breakthrough during the first PFAS removal stage. This suggests that the GAC sorbent was not as effective as the PFPE-IEX+ sorbent in removing PFAS from the leachate.

Subsequently, continuous removal of PFAS from potable water having an initial PFAS concentration at 1–2 ppb was performed and the results are illustrated in Fig. 4c and Supplementary Fig. 12. Approximate 13 litres of potable water were continuously passed through the PFPE-IEX+ cartridge for 3 days. Note that <0.1% breakthrough of all types of PFAS from C4 to C10 was observed over the 13 litres of

continuous elution, indicating that the cartridge filled with PFPE-IEX+ sorbent has high efficiency in the removal of PFAS from potable water. Furthermore, as shown in Fig. 4d for the regeneration process, PFAS with carboxylic acid charged groups (i.e. PFBA, PFPeA, PFHxA, HFPO-DA, PFHpA, PFOA, perfluorononanoic acid (PFNA), and PFDA) were washed out first during the elution process, while those having a sulfonic acid group (i.e. PFBS, PFHxS, and PFOS) were eluted later. These results demonstrate that PFPE-IEX+ cartridge is efficient in removing PFAS from both leachate and potable water.

The development of efficient and selective strategies for capturing PFAS from contaminated water sources is urgently required. The successful preparation of an environmentally stable fluorinated polymer sorbent PFPE-IEX+ lays the foundation for enhanced ability in managing PFAS contamination. The selective hydrophobic and fluorophilic interactions, combined with electrostatic attractions facilitated by ion-exchange sites, collectively contribute to its remarkable sorption performance. In comparison to conventional methods, such as activated carbon and ion-exchange resin, PFPE-IEX+ stands out as an efficient sorbent, showcasing promising performance in removing 11 PFAS compounds in real contaminated water sources. In addition, the demonstrated ability to regenerate PFPE-IEX+ through successive sorption and desorption cycles further solidifies its practical utility.

Looking to the future, the increasing demand for environmental and human health protection will heighten the need for PFAS remediation technologies. Firstly, the development of efficient and regenerable PFAS sorbents represents a promising direction. While the inclusion of PFPE segments enhances sorption selectivity, the associated high costs and PFAS-nature of PFPE may be prohibitive. Future research could explore alternatives to PFPE to reduce operational expenses and to prepare non-PFAS and even non-fluorinated sorbents. Next, controlling the size uniformity and morphology of PFAS sorbents may be crucial for achieving better quality control during scale-up synthesis processes. Finally, there is significant interest within the community in developing effective PFAS destruction technologies to prevent environmental release. Therefore, the development of a combined strategy for PFAS capture and destruction/utilization is preferable for more complete and comprehensive PFAS management.

Methods

Equilibrium PFAS removal

Different type of PFAS were spiked into potable water and leachate solutions with each PFAS having initial concentrations of 1–2 ppb and 1–10 ppb, respectively. A total of 3 mL of the filtrate solution was mixed individually with 15 mg of PFPE-IEX+ in a polypropylene vial, with the concentration of PFPE-IEX+ being 5 mg mL^{-1}. After shaking for predetermined time of 24 h on a shaker, 2 mL of each of the solution mixture was collected. For each sample, 1.5 mL of the supernatant was collected for LC-MS/MS analysis. The experiments were measured repeatedly for three times ($n = 3$).

Sorption kinetics of PFAS

For simulated PFAS-contaminated water, 11 different PFAS were respectively spiked into Milli-Q water and created an initial concentration of 10 ppb for each of the PFAS. In a polypropylene bottle, weigh 20 mg PFPE-IEX+ and add 20 mL Milli-Q water containing 11 PFAS. The final concentration of the polymer was 1 mg mL^{-1}. For real PFAS-contaminated water, 11 different PFAS were respectively spiked into leachate solutions and created an initial concentration of 1 ppb for each of the PFAS. In a polypropylene bottle, weigh 10 mg or 100 mg PFPE-IEX+ and add 20 mL leachate containing 11 PFAS, respectively. The final concentration of the polymer was 0.5 or 5 mg mL^{-1}. At each predetermined time of 0.5, 1, 3, 5, 10, 30 min, 1 and 2 h, 2 mL of the solution mixture was collected and directly centrifuged at 12,000 ppm for 15 min, 1.5 mL of the supernatant was collected for LC-MS/MS analysis for each sample. Control experiments without the presence of PFPE-IEX+ were also performed under identical conditions.

Sorption kinetics data were fitted using Weber-Morris model:

$$q_t = k_i t^{0.5} + C \quad (1)$$

Where q_t is the sorption capacity at incubation time h (min), k_i is the diffusion rate constant (μg (g x $min^{0.5})^{-1}$), C denotes the boundary layer thickness, k_i and C are the slope and intercept of the linear plot of q_t vs. $t^{0.5}$.

Sorption isotherms of HFPO-DA

The sorption isotherm of HFPO-DA was studied using PFPE-IEX+ as the sorbent. A series concentration of HFPO-DA stock solutions, with the initial concentrations of 0.2, 1, 5, 10, 20, 40 and 100 ppm were prepared in Milli-Q water. In a polypropylene vial, 6 mL of Milli-Q water was added to disperse 1.2 mg PFPE-IEX+ on a shaker for 3 h. Aliquots of 2 mL of the dispersed PFPE-IEX+ solution was added to mix with another 2 mL of the prepared HFPO-DA stock solutions. The final concentration of the polymer was 0.1 mg mL^{-1} for each solution and the concentrations of the HFPO-DA solutions were 0.1, 0.5, 2.5, 5, 10, 20 and 50 ppm respectively. The solution mixtures were placed on a shaker for 24 h, followed by magnetic separation for 10 min. For each sample, 1.5 mL of the supernatant was collected for LC-MS/MS analysis. Serial dilutions were conducted to dilute all of the samples to a final concentration of HFPO-DA to 50 ppb, with 0.1 ppm diluted two times, 0.5 ppm diluted ten times, 2.5 ppm diluted 50 times, 5 ppm diluted 100 times, 10 ppm diluted 200 times, 20 ppm diluted 400 times and 50 ppm diluted 1000 times. Control experiments without addition of PFPE-IEX+ were conducted under identical conditions.

Data were fitted using the two models below:

Langmuir isotherm model:

$$q_e = q_m \frac{K_L C_e}{1 + K_L C_e} \quad (2)$$

Freundlich isotherm model:

$$q_e = k_F C_e^{\frac{1}{n}} \quad (3)$$

The residual concentration of PFAS at equilibrium is represented by C_e (mg L^{-1}), while q_e (mg g^{-1}) is the amount of PFAS that the sorbent binds at equilibrium. q_m (mg g^{-1}) is the maximum sorption capacity, K_L (L mg^{-1}) is the Langmuir equilibrium constant representing binding affinity, while K_F ((mg g^{-1})(L $mg^{-1})^{1/n}$) is the Freundlich constant and n is the intensity of sorption.

Maximum sorption capacity of PFPE-IEX+

The individual capacity of eight different PFAS of PFPE-IEX+ was determined using ^{19}F NMR spectroscopy. The sorbent concentration used was 0.2 mg mL^{-1}, while each PFAS compound was at a concentration of 0.4 mg mL^{-1} in Milli-Q water. The sorption duration was set at 24 h. After the sorption period, 1.5 mL of the solution was taken and centrifuged at 2700 g for 15 min to ensure complete recovery of the sorbent at the bottom of the Eppendorf tube. The supernatant was then collected and analyzed using ^{19}F NMR spectroscopy. Each experiment was repeated three times, and the average values were calculated.

Regeneration ability of PFPE-IEX+

1% sodium chloride methanol solution was used for release of the sorbed PFAS. The regeneration of PFPE-IEX+ was tested for five cycles. In a typical cycle for single HFPO-DA regeneration, 1.5 mL of 1 mg mL^{-1} of HFPO-DA solution dissolved in Milli-Q water was directly added into

an Eppendorf tube (polypropylene, 1.5 mL maximum capacity) with 7.5 mg PFPE-IEX+. The solution mixture was shaken on a shaker for 30 min and then centrifuged at 8050 g for 15 min to fully recover the sorbent at the bottom of the Eppendorf tube. 1 mL of the supernatant was collected, diluted 10 times using Milli-Q water for LC-MS/MS analysis. Rest of 0.5 mL of the residue liquid was thoroughly removed using a pipette and 1.5 mL of the above prepared 1% NaCl in methanol solution was added to redisperse the sorbent on the shaker for 10 min, followed by 5 min of centrifugation at 8,050 g. 1 mL of the supernatant of 1% NaCl in methanol solution was collected, diluted 100 times using Milli-Q water and taken for LC-MS/MS analysis. The residue 0.5 mL of methanolic ammonium acetate solution was carefully removed again using a pipette. The cycle was repeated five times. The initial HFPO-DA stock solution was also collected, centrifuged under identical conditions, and diluted 100 times using Milli-Q water for LC-MS/MS analysis.

Continuous PFAS removal and regeneration in a cartridge

The experiment aimed to compare the effectiveness of two different sorbents, PFPE-IEX+ and GAC, in removing PFAS from leachate and potable water. The sorbents were contained within a column made of medical-grade polypropylene (PP), with specific dimensions: cartridge length of 115.1 mm and cartridge inner diameter (ID) of 12.8 mm. The first step involved the preparation of the sorbents, with ~ 2 g of each sorbent carefully packed into the column. Subsequently, the sorbents were subjected to three cycles of PFAS removal and regeneration to assess their initial performance and regenerability. After that, a continuous water flow was maintained, with ~ 13 liters of both leachate and potable water passed through the column at a controlled flow rate of ~ 3 mL min^{-1}. The concentrations of PFAS in the water samples were measured before the experiments, and the leachate had PFAS concentrations ranging from 1–10 ppb, while the potable water had a PFAS concentration of 1–2 ppb. For sorbent regeneration, a 1% sodium chloride solution in methanol was employed. The results of this study would offer valuable insights into the sorbents' capabilities in removing PFAS from different water sources, contributing to advancements in water treatment and environmental remediation technologies.

Data availability

The data supporting the findings of this work are available in the Supplementary Information/Source Data file. Additional data are available from the corresponding author upon request. Source data are provided with this paper.

References

1. Wang, Y. et al. Fluorination in advanced battery design. *Nat. Rev. Mater.* **9**, 119–133 (2024).
2. Fu, C. et al. Low-fouling fluoropolymers for bioconjugation and in vivo tracking. *Angew. Chem. Int. Ed.* **132**, 4759–4765 (2020).
3. Forgham, H. et al. Multifunctional fluoropolymer-engineered magnetic nanoparticles to facilitate blood-brain barrier penetration and effective gene silencing in medulloblastoma. *Adv. Sci.* **11**, e2401340 (2024).
4. Lundquist, N. A. et al. Polymer supported carbon for safe and effective remediation of PFOA-and PFOS-contaminated water. *ACS Sustain. Chem. Eng.* **7**, 11044–11049 (2019).
5. He, Y., Cheng, X., Gunjal, S. J. & Zhang, C. Advancing PFAS sorbent design: mechanisms, challenges, and perspectives. *ACS Mater. Au.* **2**, 108–114 (2023).
6. Zhang, C. et al. Biological utility of fluorinated compounds: from materials design to molecular imaging, therapeutics and environmental remediation. *Chem. Rev.* **122**, 167–208 (2021).
7. Cantoni, B., Turolla, A., Wellmitz, J., Ruhl, A. S. & Antonelli, M. Perfluoroalkyl substances (PFAS) adsorption in drinking water by granular activated carbon: influence of activated carbon and PFAS characteristics. *Sci. Total Environ.* **795**, 148821 (2021).
8. Dixit, F., Dutta, R., Barbeau, B., Berube, P. & Mohseni, M. PFAS removal by ion exchange resins: A review. *Chemosphere* **272**, 129777 (2021).
9. Buckley, T. et al. Effect of different co-foaming agents on PFAS removal from the environment by foam fractionation. *Water Res.* **230**, 119532 (2023).
10. Ross, I. et al. A review of emerging technologies for remediation of PFASs. *Remediation* **28**, 101–126 (2018).
11. Oyetade, O. A., Varadwaj, G. B. B., Nyamori, V. O., Jonnalagadda, S. B. & Martincigh, B. S. A critical review of the occurrence of perfluoroalkyl acids in aqueous environments and their removal by adsorption onto carbon nanotubes. *Rev. Environ. Sci. Biotechnol.* **17**, 603–635 (2018).
12. Olvera-Vargas, H., Wang, Z., Xu, J. & Lefebvre, O. Synergistic degradation of GenX (hexafluoropropylene oxide dimer acid) by pairing graphene-coated Ni-foam and boron doped diamond electrodes. *Chem. Eng. J.* **430**, 132686 (2022).
13. Park, M., Daniels, K. D., Wu, S., Ziska, A. D. & Snyder, S. A. Magnetic ion-exchange (MIEX) resin for perfluorinated alkylsubstance (PFAS) removal in groundwater: roles of atomic charges for adsorption. *Water Res.* **181**, 115897 (2020).
14. Hearon, S. E. et al. Montmorillonite clay-based sorbents decrease the bioavailability of per-and polyfluoroalkyl substances (PFAS) from soil and their translocation to plants. *Environ. Res.* **205**, 112433 (2022).
15. Ameduri, B. Fluoropolymers as unique and irreplaceable materials: challenges and future trends in these specific per or polyfluoroalkyl substances. *Molecules* **28**, 7564 (2023).
16. Garg, S. et al. Remediation of water from per-/poly-fluoroalkyl substances (PFAS)–challenges and perspectives. *J. Environ. Chem. Eng.* **9**, 105784 (2021).
17. Meng, P. et al. Efficient removal of perfluorooctane sulfonate from aqueous film-forming foam solution by aeration-foam collection. *Chemosphere* **203**, 263–270 (2018).
18. Kumarasamy, E., Manning, I. M., Collins, L. B., Coronell, O. & Leibfarth, F. A. Ionic fluorogels for remediation of per-and polyfluorinated alkyl substances from water. *ACS Cent. Sci.* **6**, 487–492 (2020).
19. Xiao, L. et al. β-Cyclodextrin polymer network sequesters perfluorooctanoic acid at environmentally relevant concentrations. *J. Am. Chem. Soc.* **139**, 7689–7692 (2017).
20. Tan, X. et al. Revealing the molecular-level interactions between cationic fluorinated polymer sorbents and the major PFAS pollutant PFOA. *Macromolecules* **55**, 1077–1087 (2022).
21. Tan, X. et al. Amphiphilic perfluoropolyether copolymers for the effective removal of polyfluoroalkyl substances from aqueous environments. *Macromolecules* **54**, 3447–3457 (2021).
22. O'Connor, J. et al. Distribution, transformation and remediation of poly-and per-fluoroalkyl substances (PFAS) in wastewater sources. *Process Saf. Environ. Prot.* **164**, 91–108 (2022).
23. Manning, I. M. et al. Hydrolytically stable ionic fluorogels for high-performance remediation of per-and polyfluoroalkyl substances (PFAS) from natural water. *Angew. Chem. Int. Ed.* **134**, e202208150 (2022).
24. Faucitano, A., Buttafava, A., Comincioli, V., Marchionni, G. & Pasquale, R. D. Kinetic modelling of the low-temperature photo-oxidation of hexafluoropropene. *J. Phys. Org. Chem.* **4**, 293–300 (1991).
25. Bunyard, W. C., Romack, T. J. & DeSimone, J. M. Perfluoropolyether synthesis in liquid carbon dioxide by hexafluoropropylene photooxidation. *Macromolecules* **32**, 8224–8226 (1999).
26. Kasai, P. H. Perfluoropolyethers: intramolecular disproportionation. *Macromolecules* **25**, 6791–6799 (1992).
27. Zhou, Z. et al. Molded, high surface area polymer electrolyte membranes from cured liquid precursors. *J. Am. Chem. Soc.* **128**, 12963–12972 (2006).

28. Espiritu, R., Golding, B. T., Scott, K. & Mamlouk, M. Degradation of radiation grafted hydroxide anion exchange membrane immersed in neutral pH: removal of vinylbenzyl trimethylammonium hydroxide due to oxidation. *J. Mater. Chem.* **5**, 1248–1267 (2017).
29. Herranz, D. et al. Application of crosslinked polybenzimidazole-poly (vinyl benzyl chloride) anion exchange membranes in direct ethanol fuel cells. *Membranes* **10**, 349 (2020).
30. Nhung, L. T. T., Kim, I. Y. & Yoon, Y. S. Quaternized chitosan-based anion exchange membrane composited with quaternized poly (vinylbenzyl chloride)/polysulfone blend. *Polymers* **12**, 2714 (2020).
31. Chrysostomou, V. et al. Hydrophilic random cationic copolymers as polyplex-formation vectors for DNA. *Materials* **15**, 2650 (2022).
32. Buck, R. C. et al. Perfluoroalkyl and polyfluoroalkyl substances in the environment: terminology, classification, and origins. *Integr. Environ. Assess. Manag.* **7**, 513–541 (2011).
33. Brendel, S., Fetter, É., Staude, C., Vierke, L. & Biegel-Engler, A. Short-chain perfluoroalkyl acids: environmental concerns and a regulatory strategy under REACH. *Environ. Sci. Eur.* **30**, 1–11 (2018).
34. Lin, Z.-W., Wang, J., Dyakiv, Y., Helbling, D. E. & Dichtel, W. R. Structural features of styrene-functionalized cyclodextrin polymers that promote the adsorption of perfluoroalkyl acids in water. *ACS Appl. Mater. Interfaces* **16**, 28409–28422 (2024).
35. Yang, A., Ching, C., Easler, M., Helbling, D. E. & Dichtel, W. R. Cyclodextrin polymers with nitrogen-containing tripodal cross-linkers for efficient PFAS adsorption. *ACS Mater. Lett.* **2**, 1240–1245 (2020).
36. Wang, W., Zhou, S., Jiang, X., Yu, G. & Deng, S. Fluorinated quaternary ammonium covalent organic frameworks for selective and efficient removal of typical per-and polyfluoroalkyl substances. *Chem. Eng. J.* **474**, 145629 (2023).
37. Langmuir, I. The adsorption of gases on plane surfaces of glass, mica and platinum. *J. Am. Chem. Soc.* **40**, 1361–1403 (1918).
38. Zhang, C., Sui, J., Li, J., Tang, Y. & Cai, W. Efficient removal of heavy metal ions by thiol-functionalized superparamagnetic carbon nanotubes. *Chem. Eng. J.* **210**, 45–52 (2012).
39. Parida, K., Sahu, S., Reddy, K. & Sahoo, P. A kinetic, thermodynamic, and mechanistic approach toward adsorption of methylene blue over water-washed manganese nodule leached residues. *Ind. Eng. Chem. Res.* **50**, 843–848 (2011).
40. Kamaruddin, N. H., Bakar, A. A. A., Mobarak, N. N., Zan, M. S. D. & Arsad, N. Binding affinity of a highly sensitive Au/Ag/Au/chitosan-graphene oxide sensor based on direct detection of Pb^{2+} and Hg^{2+} ions. *Sensors* **17**, 2277 (2017).
41. Vakili, M. et al. Removal of GenX by APTES functionalized diepoxyoctane cross-linked chitosan beads. *J. Environ. Chem. Eng.* **11**, 110539 (2023).
42. Huang, P.-J. et al. Reusable functionalized hydrogel sorbents for removing long-and short-chain perfluoroalkyl acids (PFAAs) and GenX from aqueous solution. *ACS Omega* **3**, 17447–17455 (2018).
43. Tan, X. et al. Efficient removal of perfluorinated chemicals from contaminated water sources using magnetic fluorinated polymer sorbents. *Angew. Chem. Int. Ed.* **61**, e202213071 (2022).
44. Ateia, M., Alsbaiee, A., Karanfil, T. & Dichtel, W. Efficient PFAS removal by amine-functionalized sorbents: critical review of the current literature. *Environ. Sci. Technol. Lett.* **6**, 688–695 (2019).
45. Wan, H. et al. Rapid removal of PFOA and PFOS via modified industrial solid waste: mechanisms and influences of water matrices. *Chem. Eng. J.* **433**, 133271 (2022).
46. Park, M. et al. Adsorption of perfluoroalkyl substances (PFAS) in groundwater by granular activated carbons: Roles of hydrophobicity of PFAS and carbon characteristics. *Water Res.* **170**, 115364 (2020).

Acknowledgements

The authors acknowledge the Australian Research Council (LP220100036, C.Z.; CE230100017, A.K.W.), the United States Army International Technology Center-Pacific (ITC-PAC, C.Z.) and The University of Queensland Knowledge Exchange & Translation Grants (DVCR23116A, C.Z.) for funding of this research. C.Z. acknowledges the Australian Research Council for his Discovery Early Career Researcher Award fellowship (DE230101105). The Australian National Fabrication Facility, Queensland Node is acknowledged for access to some items of equipment.

Author contributions

All authors participated in the results discussion, collectively advancing the progress of this research. Z.Y. synthesized the PFPE-IEX+ resins, conducted various characterizations, stability tests, PFAS sorption experiments, and played a key role in PFAS removal from real contaminated water and PFAS continuous removal and regeneration experiments. X.T. provided essential assistance and guidance throughout the entire experimental process. S.J.G. conducted the swelling ratio test, providing necessary data for the research. Y.Z., R.X. and Y.W. conducted and analyzed scanning electron microscopy, contributing to the material characterization of the research. P.D., C.F., K.L., K.M., L.G.S., L.L., T.E.H., K.V.T., J.G. and A.K.W. contribute to the discussion of experimental design and data explanation. C.Z. designed, supervised, and managed the entire project, demonstrating leadership.

Competing interests

The authors declare no competing interests.

Additional information

Supplementary information The online version contains supplementary material available at https://doi.org/10.1038/s41467-024-52690-y.

Correspondence and requests for materials should be addressed to Cheng Zhang.

Peer review information *Nature Communications* thanks Carsten Prasse and the other, anonymous, reviewers for their contribution to the peer review of this work. A peer review file is available.